ORIGINAL PAPER

Application of numerical modeling for groundwater flow and contaminant transport analysis in the basaltic terrain, Bagalkot, India

G. Tamma Rao · V. V. S. Gurunadha Rao ·
L. Surinaidu · J. Mahesh · G. Padalu

Abstract A three-dimensional steady-state finite difference groundwater flow model is used to quantify the groundwater fluxes and analyze the subsurface hydrodynamics in the basaltic terrain by giving particular emphasis to the well field that supplies domestic, agricultural, and industrial needs. The alluvial aquifer of the Ghatprabha River comprises shallow tertiary sediment deposits underlain by peninsular gneissic complex of Archean age, located in the central–eastern part of the Karnataka in southern India. Integrated hydrochemical, geophysical, and hydrogeological investigations have been helped in the conceptualization of groundwater flow model. Hydrochemical study has revealed that groundwater chemistry mainly controlled by silicate weathering in the study area. Higher concentration of TDS and NO_3-N are observed, due to domestic, agriculture, and local anthropogenic activities are directed into the groundwater, which would have increased the concentration of the ions in the water. Groundwater flow model is calibrated using head observations from 23 wells. The calibrated model is used to forecast groundwater flow pattern, and anthropogenic contamination migration under different scenarios. The result indicates that the groundwater flows regionally towards the south of catchment area and the migration of contamination would be reached in the nearby well field in less than 10 years time. The findings of these studies are of strong relevance to addressing the groundwater pollution due to indiscriminate disposal practices of hazardous waste in areas located within the phreatic aquifer. This study has laid the foundation for developing detailed predictive groundwater model, which can be readily used for groundwater management practices.

Introduction

The water demand for industrial, agricultural, and domestic uses is continuously increasing and freshwater resources are shrinking. Against this backdrop, groundwater management is a critical issue for current and future generations. Groundwater management entails both quantity and quality-related groundwater resource management.

Geochemical methods are commonly applied to study groundwater flow regimes (Anderson and Woessner 1992). Groundwater models play an important role in the development and management of groundwater resources and in predicting effects of management measures. With rapid increases in computation power and the wide availability of computers and model software, groundwater modeling has become a standard tool for professional hydrogeologists to effectively perform most tasks. There is a lot of research on pollution in urban environment which is mostly focused on

G. Tamma Rao (✉) · V. V. S. Gurunadha Rao · L. Surinaidu ·
J. Mahesh · G. Padalu
National Geophysical Research Institute,
(Council of Scientific & Industrial Research),
Uppal Road,
Hyderabad 500 606, India
e-mail: gopingri@gmail.com

groundwater quality statistics (Vidal et al. 2000; Foppen 2002; Shepherd et al. 2006; Bakri et al. 2008).

A large range of tools for integrated urban water management (IUWM) are available and recently, 65 different IUWM models were compared (Mitchell et al. 2007). However, the models are not suited to depicting the variations in groundwater levels or the qualitative deterioration of urban groundwater as they include no information on regional groundwater flow fields or aquifer characteristics (Wolf 2007). Changes of groundwater recharge due to urbanization and its effect on groundwater level was studied by Gobel et al. (2004) and Jat et al. (2009). The study proceeded with the development of the conceptual model of regional groundwater flow. The study presented herein used processing MODFLOW and the solute transport code (MT3D) to construct a groundwater flow model and to model contaminant transport in the basin. The calibration of the model parameters was conducted under steady-state flow conditions. The numerical model was then used to simulate the groundwater flow under the current stress conditions.

These models were then used as a management tool for assessing the current situation and forecasting future responses to assumed coming events. A combination of field research and the application of the integrated peri-urban water management model series were applied this study area. This research was the first application of an integrated approach of investigation of the whole rural water cycle in a selected pilot area in basaltic terrain in order to estimate the impact of the peri-urban area to the underlying aquifer.

Study area

An Organo Chemical Unit is located on a ridge at Sameerwadi village, spread over about 48 km^2 in the basaltic terrain, Bhagalkot district, Karnataka, India (Fig. 1). Two prominent streams drain the watersheds through Munyal and another one through Dhavaleshwar and the two streams join Ghataprabha River in the south. The Munyal distributary and Dhavaleshwar distributaries of

Fig. 1 Location map of study area, Bagalkot District, Karnataka
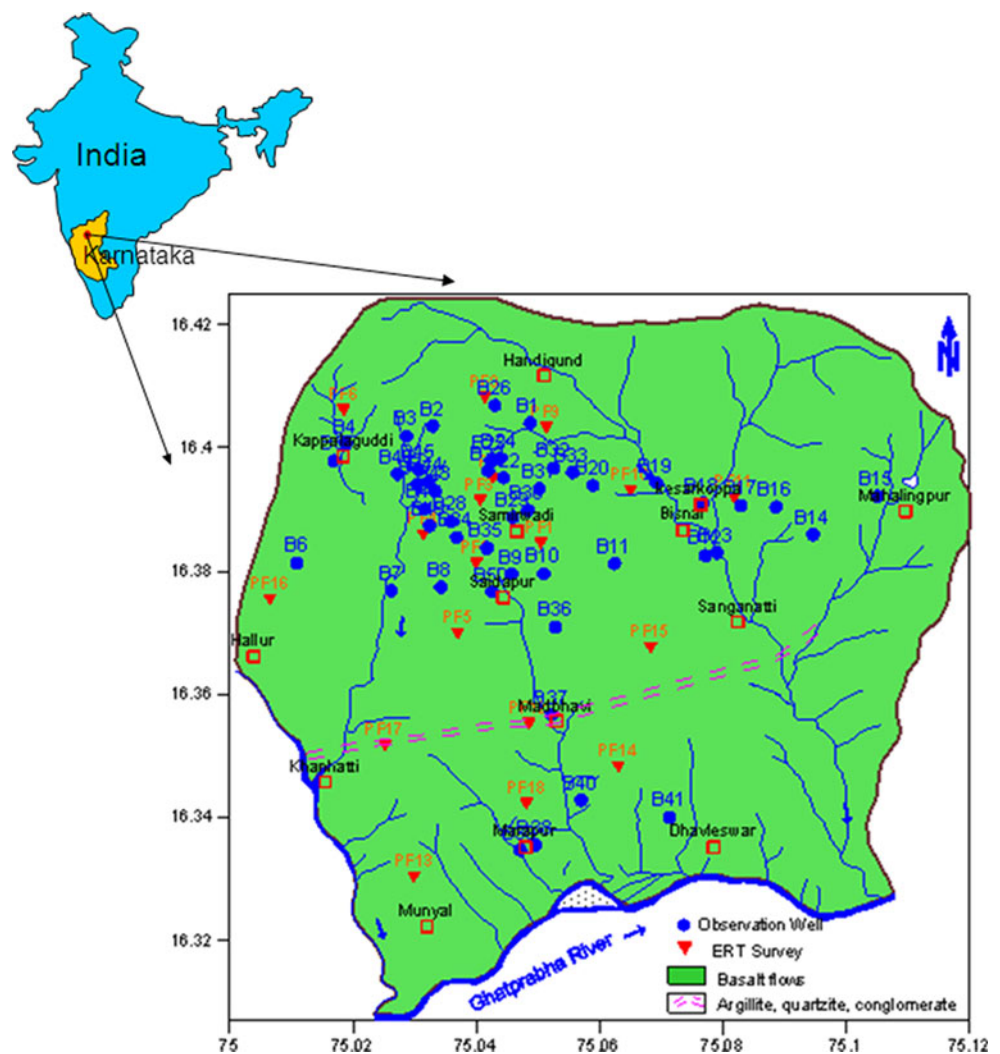
Ghataprabha left branch canal are ridge canals and surface water irrigation channels are drawn on both sides of the ridge. The climate of the district as a whole can be termed as semi-arid. The area experiences the rainfall ranging between 600 and 800 mm/annum. The variation in the maximum temperature during the year ranges from 27°C to 35.7°C and minimum from 13.9°C to 20.6°C (Mahesha and Prasannakumar 1989). The study area experiences pleasant winters and hot dry summers. The hot season extends from March to May, during which the daily maximum temperature often shoots up to 35.7°C. Black cotton soil is the dominant soil type in the area (Fig. 2). Most of the study area is arable land and followed by fallow and pasture land (GSI 1991; Fig. 3).

Geology

Groundwater flow in basaltic aquifers takes place mainly through open fractures and joints (Domenico and Schwartz 1990). In the unsaturated zone, the flow is preferential, mainly through connective fractures. In the study area, the basalt flows cover the entire study area with intrusions of argillite, quartzite, and conglomerate between Khanahatti and Sanganahatti villages. Isolated capping of laterite occurs at several places on Deccan Traps. The sediments of Kaladgi super group are divisible into lower Bagalkot group and Upper Badami group. The stratigraphy sequence of the Bagalkot District is shown in Table 1. The lithofacies

such as conglomerates–quartzite–argillite, dolomite, limestone, chert argillite are common and these sequence repeated in cycles to form different formations. The Deccan basaltic flows occupy the area to the north of Krishna River and partially cover the rocks of Kaladgi and Dharwar super groups. The northern part of the district is characterized by plateaus and denudation slopes on Deccan Basalt (GSI 1991). The sedimentary rocks gave given rise to gentle slopes in the study area (Fig. 4).

Hydrogeology

Groundwater occurrence in the area is governed by contrasting water-bearing properties of different basaltic flows. In Deccan traps weathered zones, jointed and fractured units in the massive and vesicular basalts form the important water bearing zones horizons (GSI 1991). Weathering is noticed from 3 m to more than 20 m depth. Sand and alluvium of recent origin are seen along the major streams, which are derived from granite, gneiss, and sandstone rocks (Mahesha and Prasannakumar 1989). Groundwater level contours indicated that the groundwater flow direction is from Handigud–Kesarkoppa–Bisnal to Sanganatti in the Dhavaleshwar watershed (Fig. 5). The groundwater occurs under water table condition within shallow depths and semiconfined to confined conditions in the vesicular and jointed horizons at deeper levels. Its occurrence and movement is governed by topography,

Fig. 2 Soil map of the study area
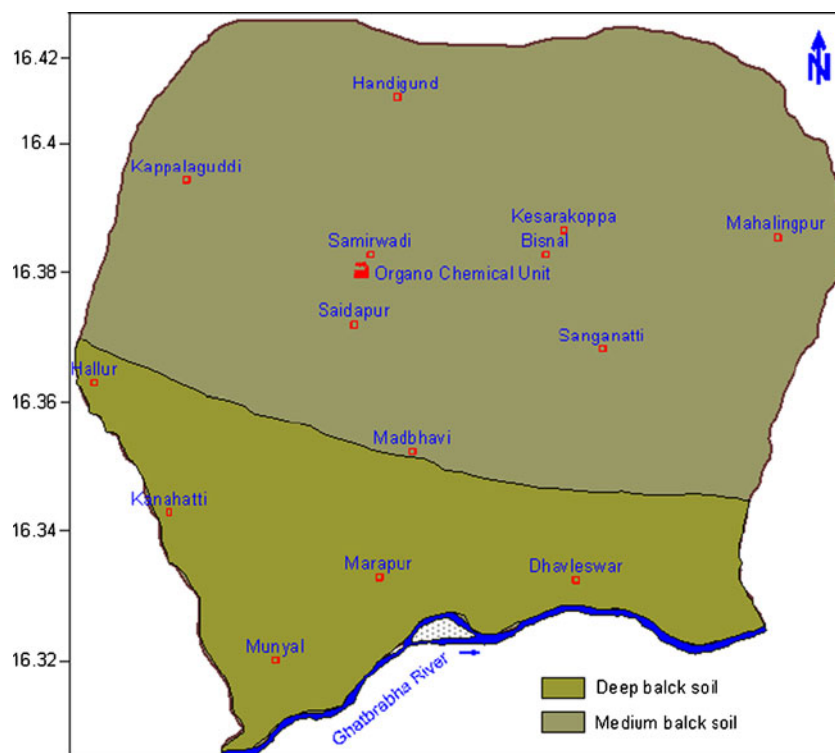
Fig. 3 Land use map of the study area
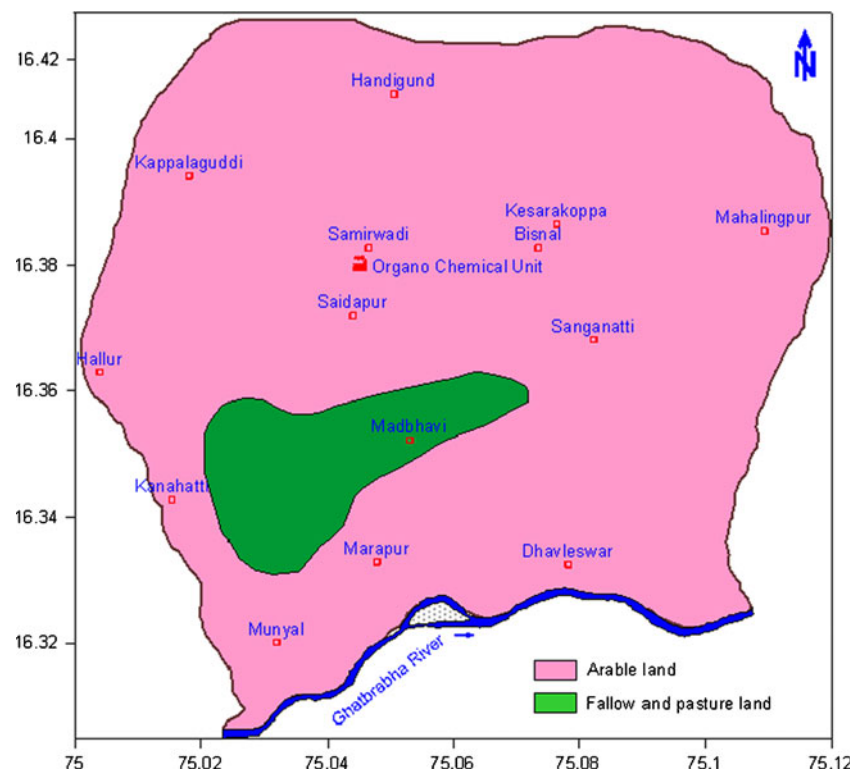
nature of aquifer like extent of weathering and fracture pattern, thickness, and extent of vesicular basalts. The highest elevation is north of Sameewadi at 585 m and lowest elevation is 545 m close to Ghataprabha River. The drainage pattern is dendritic to subdendritic and most of the tributaries are influent in nature, while the Ghataprabha River is effluent. The distributaries of Ghataprabha left bank canal along the ridge and irrigates one crop. The maximum depth to groundwater level is varying from 20 to 24 m (bgl) around the Organo chemicals in the Munyal watershed during premonsoon whereas the depth to groundwater level ranged from 8 to 12 m around Bisnal village. Present deep groundwater table condition due to overexploitation of groundwater could be attributed to the groundwater flow pattern towards Saidapur village. The Munyal distributary and Dhavaleshwar distributaries of Ghataprabha left branch canal are ridge canals and surface water irrigation channels are drawn on both sides of the ridge.

Material and methods

Sampling and measurement techniques

Groundwater samples were collected after well inventory survey from 47 representative wells during July 2007 (Fig. 1). The samples were collected after 10 min of pumping and stored in polyethylene bottles at 4°C

following the American Public Health Association (1995). The sampling bottles were rinsed thoroughly with sampled groundwater. The water samples from bore wells were collected after pumping out water for about 10 min to remove stagnant water from the well (Singh et al. 2011). Immediately after sampling, pH and electrical conductivity (EC) were measured in the field. Total dissolved solids (TDS) were calculated from EC multiplied by 0.64 (Brown et al. 1970). EC, pH, chloride, and nitrate were analyzed using multiple parameters ion meter model Thermo Orion 5 Star. Sulfate, was measured using a double beam UV–vis spectrophotometer model PerkinElmer Lambda 35 by turbidimetric, stannous chloride, molybdosilicate, and colorimetric methods, respectively. Sodium, potassium, and calcium were analyzed using flame photometer model CL-378 (Elico, India). Total carbonate and bicarbonate alkalinities were measured by acid–base titration.

Geophysical investigations

Geophysical investigations have been carried out in the watershed and data has been used for the development of groundwater flow and mass transport model for prognosing the impact of contaminant migration in groundwater around the industry. Electrical resistivity tomography (ERT) which is a non-invasive method is extremely useful for understanding the subsurface formations and for depth estimations of natural resources. IRIS-make SYSCAL PRO-96 System, which

Table 1 Stratigraphy sequence of the Bagalkot District

LITHOLOGY	FORMATION	GROUP
Laterite		
Basalt flows		
Limestone	Shahabad Formation	Bhima Group
Shale, sandstone, conglomerate	Rabanapalli Formation	
Lime stone, shale	Kotageri Formation	Badami Group
Arenite, conglomerate	Kerur Formation	
…………… Angular unconformity……………		
Argillite	Hosakatti Formation	Simikeri sub-Group
Dolomite,banded hematite, Chert breccia	Arlikatti Formation	
Argilit,quartzite, conglomerate.	Kundargi Formation	
………… Disconformity……………		
Argillite	Yadahalli Formation	Lokapur sub-Group
Dolamite, limestone, argillite	Muddapur Formation	
Dolamite, limestone, argillite	Yendigeri Formation	
Dolamite, argilite, chert	Yergatti Formation	
Argilite,quartzite,conglomerate	Ramdurg Formation	
…………… Nonconformity…………		
Basic dyke		
Pink and grey granite (porphyritic and norporphyritic)	Clospet granite	
Metasediments and metavolcanoes	Hungund Metamorphics Dharwar Supergroup	
Migmatite and gneiss	Peninsular Gneissic Complex	

(Kaladgi Group; Bagalkot group comprises Simikeri sub-Group and Lokapur sub-Group)

comprises of 96 electrodes maintaining up to 5 m inter-electrode separation is used for the surveys. Eighteen locations in the watershed are useful for assessment of groundwater resources as well as delineation of aquifer geometry. Using a combination of apparent formation resistivity (Acworth 2001) and inferred depth of weathering, it is possible to characterize the various lithologies from the multi-electrode resistivity imaging profiles.

Modeling approach

To carry out this study, three-dimensional finite difference numerical models of the unconfined aquifer were developed using the US Geological Survey software: the MODFLOW groundwater code (Harbaugh et al. 2000) for simulations and mass transport model MT3DMS (Zheng and Wang 1999). Much of the effort expended in this study was directed towards developing a simple and effective groundwater flow and mass transport model. And the groundwater flow model is a representative of the main features in the study area that is important to the deeper parts of the flow system.

Hydrochemistry

The analytical results of the chemical analysis and the statistical parameters such as minimum, maximum, mean groundwater are presented in Table 2 for both premonsoon and postmonsoons. The EC ranges from 505 to 7,000 μS/cm with a mean of 1,619 and 356–5,120 μS/cm with a mean of 1,236 μS/cm for post- and premonsoon seasons. The drastic reduction in the EC concentrations is due to the rainfall recharge in the study area. It is observed that waters of high EC values are predominant with Na and Cl ions. The pH of groundwater is ranging from 6.75 to 8.12 for premonsoon and 6.95–7.8 for postmonsoon. It means that it is in the range of neutral to alkaline nature. The concentration of TDS is ranging from 323 to 4,480 and 228 to 3,277 mg/L for both premonsoon and postmonsoon, respectively. There is a considerable amount of dilution of concentration of ions during the postmonsoon due to precipitation in this period. Salts, which held back in the interstice or pores in clay/shale while groundwater is evaporated or water table falls, get leached back to the groundwater during the rainy period (Janardhan Raju

Fig. 4 Geomorphology of the study area
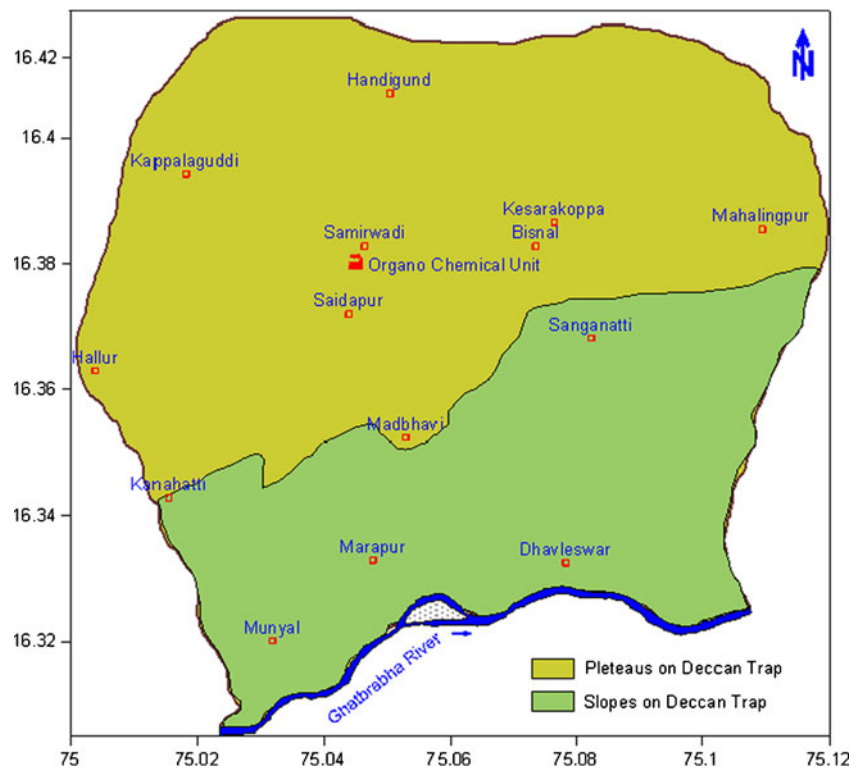
2007). Concentrations of the TDS are presented Table 3 for pre- and postmonsoon. Higher concentration of TDS and EC are observed in the study area, due to domestic effluents and local anthropogenic activities are directed into the groundwater, which would have increased the concentration of the ions in the water. Few samples are

Fig. 5 Groundwater level contours in the study area
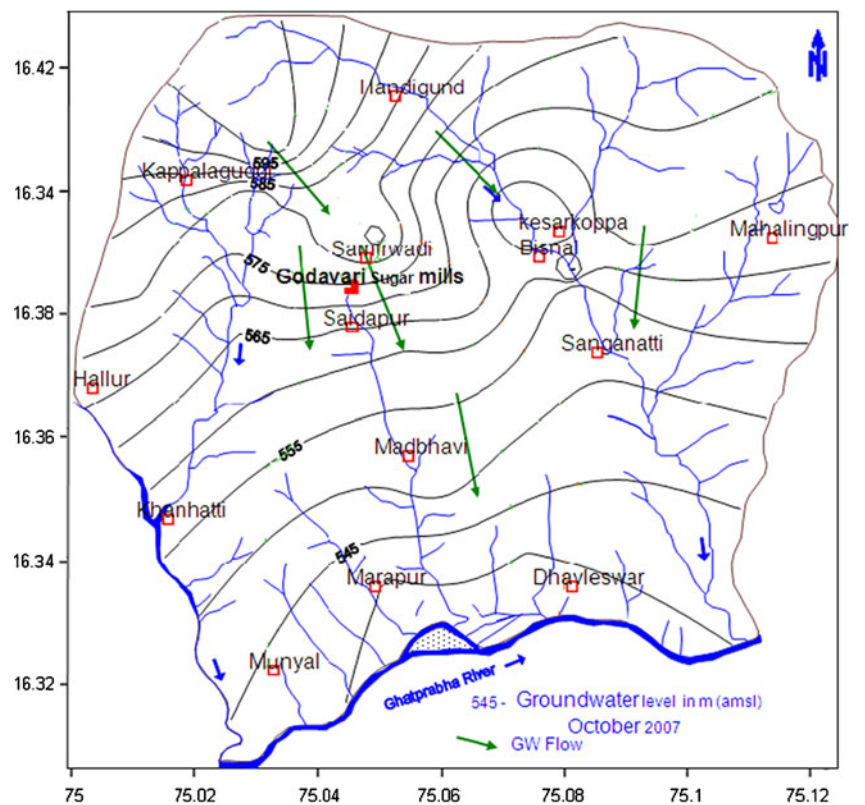
Table 2 Concentration of major ions in groundwater samples

Parameter		pH	EC μS/cm	TDS mg/L	Na meq/L	K meq/L	Ca meq/L	Mg meq/L	Cl meq/L	SO₄ meq/L	NO₃-N meq/L	HCO₃ meq/L
Pre-monsoon	Min	6.75	505	323	0.87	0.12	0.8	1.58	0.85	0.24	0.01	1.48
	Max	8.12	7,000	4,480	17.74	2.28	47.2	17	49.86	16.04	0.66	5.41
	Mean	7.4	1,619	1,036.06	3.72	0.26	6.43	5.96	7.92	3.47	0.21	3.01
Post-monsoon	Min	6.95	356	228	0.3	0,12	1.2	0.83	0.85	0.21	0.01	1.9
	Max	7.8	5,120	3,277	19.22	1.84	31.6	16.58	34.93	9.29	0.42	5.62
	Mean	7.3	1,236	791.34	3	0.22	4.8	4.3	5.28	2.26	0.16	3.27

showing increase of TDS concentrations due to mixing of surface pollutants during the infiltration and percolation of rainwater in postmonsoon season (Janardhan Raju 2007).

The higher elevations of Ca, Na, and Mg cations are due to chemical weathering of basalt minerals in both seasons (Mahesha and Prasannakumar 1989). Soils in the study area are rich in clay and bases due to hydrolysis, oxidation, and carbonation. The scatter diagram of Ca+Mg vs. HCO₃+SO₄ (Fig. 6) shows that majority samples in both the seasons fall below the equiline indicating that silicate weathering was the primary process involved in the evolution of groundwater (Srinivasamoorthy et al. 2008). If bicarbonate and sulfate are dominating than calcium and magnesium, it reflects that silicate weathering was dominating and, therefore, was responsible for the increase in the concentration of HCO₃ in groundwater (Stallard and Edmond 1983). Under suitable conditions, clay minerals may release exchangeable sodium ions. This causes higher concentration of sodium in areas where clays are found. Higher elevation of K ions in the study area due to the alteration of granetic gneisses. Since Cl is abundant in both the seasons, it might have been derived from anthropogenic sources of Cl including fertilizer, human and animal waste, and industrial applications. This is well-evidenced from Cl levels of the study area.

Table 3 TDS (mg/L) concentration

Well no.	Pre-monsoon TDS	Post-monsoon TDS	Well no.	Pre-monsoon TDS	Post-monsoon TDS
B1	323	1,043	B26	378	322
B2	755	755	B28	433	339
B3	1,389	934	B29	851	314
B4	838	742	B30	1,216	437
B5	800	922	B31	422	666
B6	419	515	B32	458	422
B7	685	605	B33	543	434
B8	487	228	B34	453	954
B9	509	612	B35	446	1,376
B10	406	426	B36	1,274	611
B11	717	560	B37	1,498	1,862
B12	2,170	781	B38	845	1,683
B13	1,248	787	B39	1,798	915
B14	386	435	B40	1,139	484
B15	646	611	B41	1,107	902
B16	448	510	B43	1,517	3,277
B17	637	723	B44	2,157	1,338
B18	966	672	B45	4,480	1,382
B19	609	864	B46	1,568	428
B20	890	11,136	B47	2,611	532
B22	685	749	B48	580	570
B23	2,003	928	B49	426	1,088
B24	1,530	336	B50	627	890
B25	2,176	438			

Fig 6 Ca+Mg versus SO₄+ HCO₃ plot for both pre-monsoon and post-monsoon
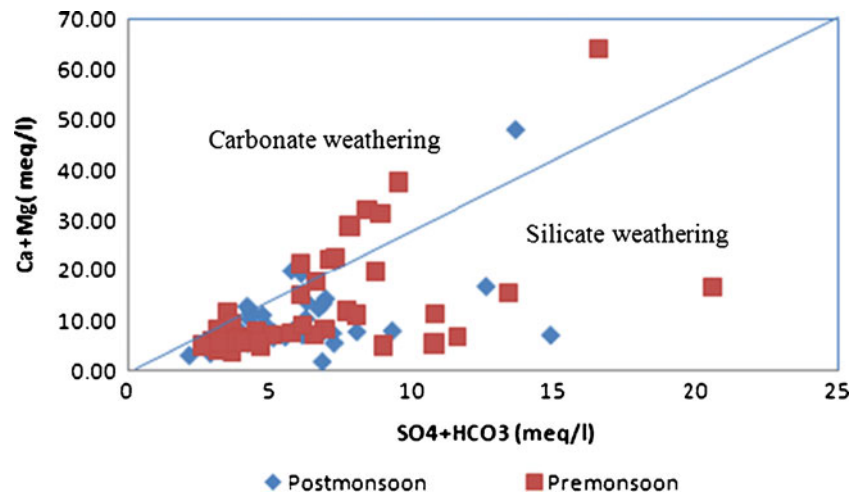
The excessive use of fertilizers in agriculture is the cause of high concentrations of groundwater NO₃-N in the study area. Significant nitrate contamination in the study area is undoubtedly the result of the overuse of fertilizers and manure on agricultural fields. Therefore, NO₃-N contamination of aquifers has been an important issue in hydrogeology and hydrochemistry over the last two decades. NO₃-N in groundwater originates largely from diffuse (nonpoint) sources in relation to diverse agricultural and domestic practices, as well as from point sources such as sewage effluents (Fogg et al. 1998). In particular, shallow aquifers in agricultural fields are highly vulnerable to nitrate contamination due to the widespread application of fertilizers and manure. There is no possibility of contaminants crossing the ridge and entering the Dhavaleshwar watershed as the predominant groundwater flow direction is towards Saidapur village. There is also intensive irrigation in the Dhavaleshwar watershed. Thus, contamination is confined to the factory premises and in the southern direction up to Saidapur village.

The Gibbs diagram is widely used to establish the relationship of water composition and aquifer lithological characteristics (Gibbs 1970, Eq. 1). The chemical composition of groundwater indicated that rock–water interaction (Elango and Kannan 2007). Three distinct fields such as precipitation dominance, evaporation dominance, and rock–water interaction dominance areas are shown in the Gibbs diagram. The predominant samples fall in the rock–water interaction dominance to evaporation dominance field of the Gibbs diagram for both monsoons (Fig. 7a, b).

$$\text{Gibbs ratio TDS vs } Na/(Na + Ca + K) \text{ for cations}$$
$$\text{and}$$
$$\text{TDS vs } Cl/(Cl + HCO_3) \text{ for anion.} \qquad (1)$$

The distribution of sample points, as shown as a cluster, suggests that the chemical weathering of rock-forming minerals and evaporation are influencing the groundwater quality. Evaporation greatly increases the concentrations of ions formed by chemical weathering, leading to higher salinity. Anthropogenic activities (agricultural fertilizers and irrigation return flows) also influence the evaporation by increasing Na and Cl, and thus TDS.

Geophysical investigations

The assigned lithology shows excellent correlation with the mapped geology and the main lithounits. ERT survey no.1 has been carried out with Wenner–Schlumberger configuration using multi-electrodes (96 electrodes) with 5-m electrode interval and the spread covering a length of 480 m, in front of the Organo chemicals. The subsurface represented by the inverse model resistivity section along the profile has been grouped into three geoelectric layers based on the variation of resistivity. In this inverse model resistivity section, the top layer has been possessing resistivity <70 ohm-m representing weathered basaltic rocks and has a thickness of about 40 m. A second layer has been identified with resistivity ranging between 100 and 150 ohm-m representative of fracture zone covering vesicular flow and it has been found continuous with an average thickness of 10–12 m. The underlying third layer has a reported resistivity of >150 ohm-m, which is a typical resistivity of basaltic rocks around Mudhol Taluk. In, general the area can be viewed as a three-layered earth model representing weathered basaltic rock, followed by vesicular zone with fracture interconnections, underlain by hard basaltic rocks, which forms the basement rock in the region. ERT image indicates that the subsurface has been more or less uniformly stratified over the entire profile except minor variations within the weathered zone at places. The resistivity >60 ohm-m represents dry soil horizon in the top, which is having a thickness of 6–9 m. The thickness of weathered zone determined in the inverse model resistivity section has been confirmed from the weathered zone thickness, which has been

Fig. 7 Gibbs diagram for both pre- and postmonsoon
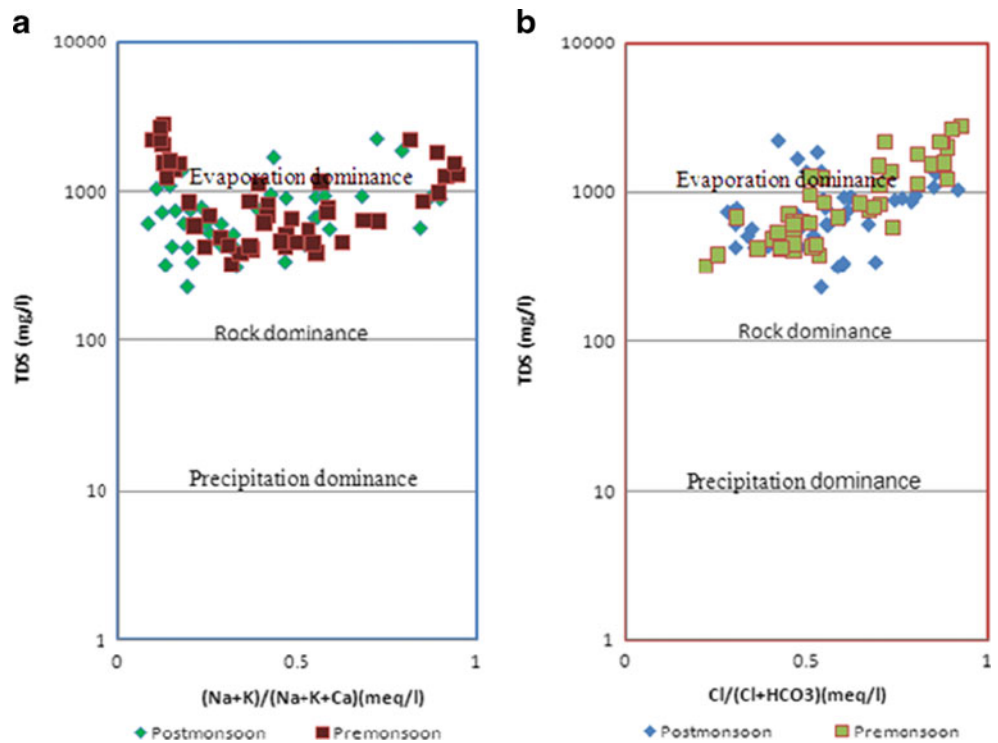
reported from lithologs of wells examined in the area. The combined thickness of weathered zone and vesicular zone could form the aquifer material through which groundwater movement occurs in the area. The ERT survey no 3 has been carried out in the compost area inside the factory premises (Fig. 8). The inverse model resistivity section indicates good groundwater potential. The weathered and vesicular zone extends up to a depth of 40 m overlain with high resistivity layer of >100 ohm-m. A low permeability layer in the top of the composting area does restrict seepage from stacked material. However, once seepage from compost enters the underlying layer, it would move faster as the resistivity is low representing a good aquifer zone. Thus, there is possibility of groundwater contaminant migration from this zone after releases from top 10 m high resistivity zone in the composting area.

Flow and transport model

Governing equations

A general form of the governing equation which describes the three-dimensional movement of groundwater flow of constant density through the porous media is (Freeze and Cherry 1979).

$$\frac{\partial}{\partial x}\left(Kx\frac{\partial h}{\partial x}\right) + \frac{\partial}{\partial y}\left(Ky\frac{\partial h}{\partial y}\right) + \frac{\partial}{\partial z}\left(Kz\frac{\partial h}{\partial z}\right) - w = Ss\frac{\partial h}{\partial t}$$
(1)

Where, Kx, Ky, and Kz are values of hydraulic conductivity along the x, y, and z coordinate axes (L/t)

h is the potentiometric head (L)
w is the volumetric flux per unit volume and represents sources and/or sinks of water per unit time (t^{-1})
S_s is the specific storage of the porous material (L^{-1}) and
t is time (t)

The first part of this problem was run to get a steady state solution that takes the form:

$$\frac{\partial}{\partial x}\left(Kx\frac{\partial h}{\partial x}\right) + \frac{\partial}{\partial y}\left(Ky\frac{\partial h}{\partial y}\right) + \frac{\partial}{\partial z}\left(Kz\frac{\partial h}{\partial z}\right) - w = 0.0$$
(2)

From the steady-state solution, the hydraulic conductivity for model aquifers can be found. Then, the equation is solved for transient case in order to solve for storage coefficient. The partial differential equation for three-dimensional transport of contaminants in groundwater is (Freeze and Cherry 1979),
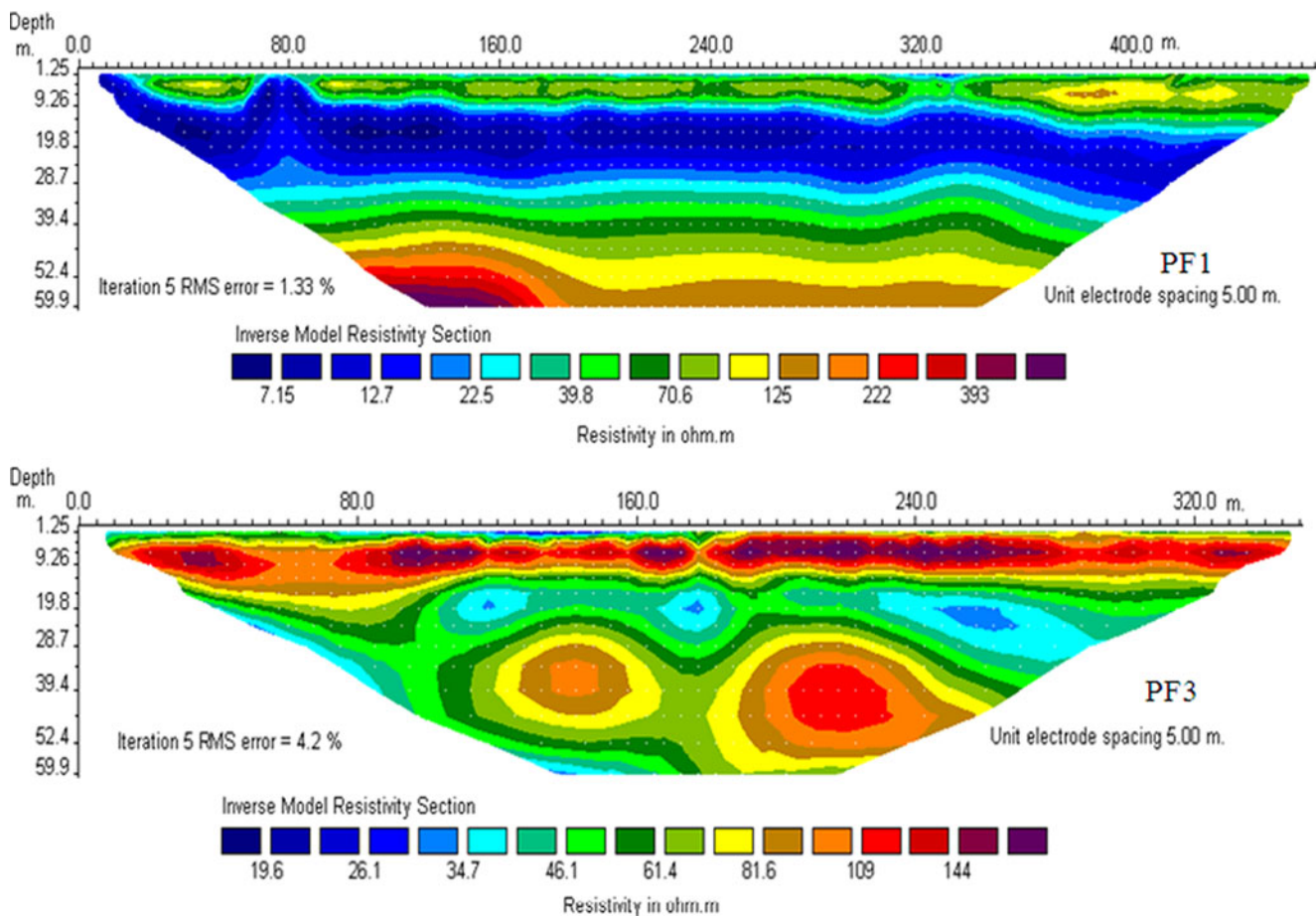
$$\frac{\partial C}{\partial t} = \frac{\partial}{\partial x_i}\left[D_{ij}\frac{\partial C}{\partial x_i}\right] - \frac{\partial}{\partial x_i}(v_i C) + \frac{q_s}{\theta}C_s + \sum_{k=1}^{N}R_k$$
(3)

where,

C the concentration of contaminant dissolved in groundwater
t time (t)
x_i the distance along the respective Cartesian co-ordinate axis

Fig. 8 ERT images in front of the factory area (*PF1*) and compost area (*PF3*)

D_{ij} the hydrodynamic dispersion coefficient

v_i the seepage or linear pore water velocity

q_s the volumetric flux of water per unit volume of aquifer representing sources (positive) and sinks (negative)

C_s the concentration of the sources or the sinks

θ the porosity of the porous medium and

R_k chemical reaction term

Model grid and parameterization

The simulated model domain of the groundwater flow model of both Munyal and Dhavaleshwar watersheds covering about 48 km^2 has been constructed using the above hydrogeological and geophysical data base. A two-layer aquifer system covering weathered and vesicular zones in the basaltic rocks have a total thickness of 55–60 m has been simulated in the model uniform grid spacing of 100×100 m has been used in the model. The model utilizes MODFLOW-2000 (Harbaugh et al. 2000) for groundwater flow as implemented in Visual MODFLOW 4.1. Active inactive regions and conductivity map of the

groundwater model domain are shown in (Fig. 9). Variable aquifer parameters assigned to five different hydrogeologic units distributed in the model are given in Table 4.

The permeability values assigned in the model varied from 2 to 3 m/day. Natural hydrological boundary condition of river has been assigned to Ghataprabha River and prominent streams around Munyal and Dhavaleshwar. A constant head boundary was simulated in the northern part to represent lateral inflow entering into the watersheds. No flow enters from the rest of the watershed boundaries. Pumping centers of water supply wells and irrigation wells have been enumerated and incorporated in the model. The average pumping rate of bore wells is about 50 m^3/day. The density of irrigation wells around the plant in Sameerwadi and Saidapur is slightly high.

Boundary conditions

Natural hydrological boundary condition of River has been assigned to Ghataprabha River and prominent streams around Munyal and Dhavaleshwar. A constant head boundary was simulated in the northern part to represent lateral inflow entering into the watersheds. The canal distributaries are

Fig. 9 Simulated weathered and fractured zones in the ground-water flow model—row 24
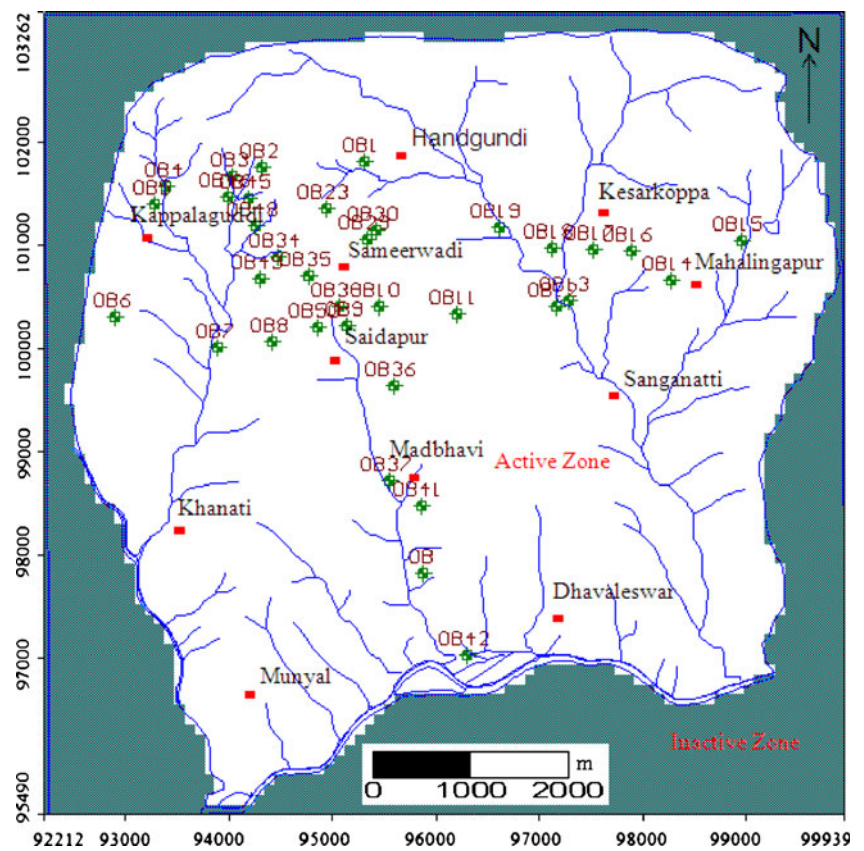
passing on the ridge between two watersheds and supply irrigation water for irrigation of dry crop during rabi season and does not contribute much to the groundwater regime. Groundwater recharge due to rainfall has been assumed as 72 mm/year for the entire area except the compost area within the plant (Rao et al. 2008). Additional input from the compost area has been simulated at a recharge rate of 100 mm/year. In general, major part of natural groundwater recharge due to rainfall may be leaving the watersheds as base flow to the streams and Ghataprabha River.

Transport model

Mass transport in three dimensions (MT3D) is a computer model for simulation of advection, dispersion, and chemical reactions of contaminants in three-dimensional groundwater flow systems (Zheng 1990). The initial conditions are set as the background concentration of TDS for the entire model domain to predict the semi-equilibrium conditions. Mass transport of total dissolved solids has been investigated by using MT3D.

The source loading from the compost area has been simulated by assigning TDS concentrations of 4,000 mg/L at the groundwater table during the 50 years of simulation. The compost area is situated close to the ridge and groundwater movement is from the compost area towards Saidapur village. The leachate from the compost area was assumed to be reaching the groundwater table with the above concentrations during the entire simulation period. The initial background average TDS concentration was assumed to be 500 mg/L.

Table 4 Variable aquifer parameters assigned to five different hydrogeologic units distributed in the model

Unit	Description	Horizontal $K_x = K_y$	Vertical K_z	Specific storage (S_s)	Specific yield (S_y)	Effective porosity
1	Block wise	3	0.2	2×10^{-4}	0.15	0.2
2	River bed	40	4	2×10^{-4}	0.15	0.2
3	Upstream	2	0.2	2×10^{-4}	0.15	0.2
4	Downstream	3	0.3	2×10^{-4}	0.15	0.2
5	streams	12	1.2	2×10^{-4}	0.15	0.2

Flow model calibration

The numerical model was calibrated under steady-state conditions through a series of groundwater flow simulations and achieved by a trial-and-error method. The conceptualization of the regional flow and the relatively complex model architecture were precisely defined in the preliminary stage of the model development. In order to constrain model results, parameters such as thickness of model layers, mesh size, boundary conditions, and hydraulic conductivities of fractured rock and solid rock units were assumed to be entirely known. With this assumption, the only parameters contributing to the uncertainty of the model simulations were: (a) the hydraulic conductivity and (b) the distribution of the areal infiltration rate. The calibration was done by comparing the simulated heads against the measured groundwater levels in fractured aquifers. The computed water level accuracy was judged by comparing the mean error, mean absolute, and root mean squared error calculated (Anderson and Woessner 1992). Root mean square error is the square root of the sum of the square of the differences between calculated and observed heads, divided by the number of observation wells, which in the present simulation is 4.948 m. The absolute residual mean is 3.996 m. During simulation, 23 observed hydraulic heads has been used for flow model. The computed vs. observed hydraulic heads at 23 observation wells were found matching closely (Table 5). The calibration parameters set in this modeling exercise are the generalized head boundary, recharge, evapotranspiration, hydraulic conductivity, specific yield, etc. The groundwater velocity field is computed from the flow model assuming an effective porosity of 0.15. The computed groundwater velocity field represents a maximum groundwater velocity of about 25 m/year.

Solute transport model calibration

The calibrated conditions were used as initial conditions for the transport model. The transport model was coupled to the flow model by velocity terms. The water level configuration of a particular time period will be considered for solving groundwater flow equation under steady state and thereby a single velocity field determined for the mass transport simulation for all times. With a small time step, this particle motion traces a path line through the system (Konikow and Bredehoeft 1978). Dispersion was accounted for in the particle motion by adding to the deterministic motion a random component, which is a function of the dispersivities. The mean concentration for each grid block was calculated as the sum of the mass carried by all the particles located in a given block divided by the total volume of water in the block. The head solution is obtained using visual MODFLOW (McDonald and Harbaugh 1988).

Table 5 Computed versus observed head values

Target no.	Observed head (m)	Calculated head (m)	Residual
OB1	562	560.40	−0.4
OB3	570	568.79	1.21
OB5	560	562.79	−2.79
OB6	544	542.22	1.78
OB8	555	553	2.0
OB10	545	547.42	2.42
OB11	553	551.34	1.66
OB12	552	552.65	−0.65
OB13	552	554.32	−2.32
OB15	533	532.03	0.97
OB17	552	551.95	0.05
OB18	555	553	2
OB23	565	566.86	−1.86
OB29	562	563.20	−1.2
OB30	551	552.75	−1.75
OB35	555	554.88	0.38
OB36	545	545.62	−0.62
OB37	536	535.30	0.7
OB38	548	547.77	0.3
OB46	555	553.51	1.49
OB48	547	548.46	−1.46
OB49	545	544.36	0.64
OB50	549	548.43	0.57

Targets are shown in Fig. 1

TDS concentration was then calculated at all node points for premonsoon, a date up to which the system was assumed to be in a steady-state condition. There was a mismatch between observed and computed values of TDS. Therefore, efforts were made to obtain a reasonably better match by modifying the magnitude and distribution of the background concentration and pollutant load. To obtain the real representation of the aquifer system, field data (postmonsoon) were considered for other steady-state condition and were also run to visualize the mass transport model. The hydraulic conductivity was changed by 20% (K_x and K_z) of the value assigned in the model at each node. Change in conductivity affects groundwater velocity, causing redistribution of solute concentration. In general, the higher the conductivity the faster is the movement of the solute. The calibrated recharge values have been divided into three zones. The extreme southern zone is assigned as 110 mm/year, inside compost area as 85 mm/year, and the extreme northern zone as 200 mm/year. But the evaporation is estimated to a maximum rate of 60 mm/year with an extinction depth of 3.0 m based on the type of crops and plants that grow in the area. The longitudinal dispersivity was increased to 50 and 200 m (from 30 m). Transverse dispersivity was taken as one third of the longitudinal dispersivity.

Fig. 10 Computed groundwater level contours in m (amsl) in the groundwater flow model—July 2007
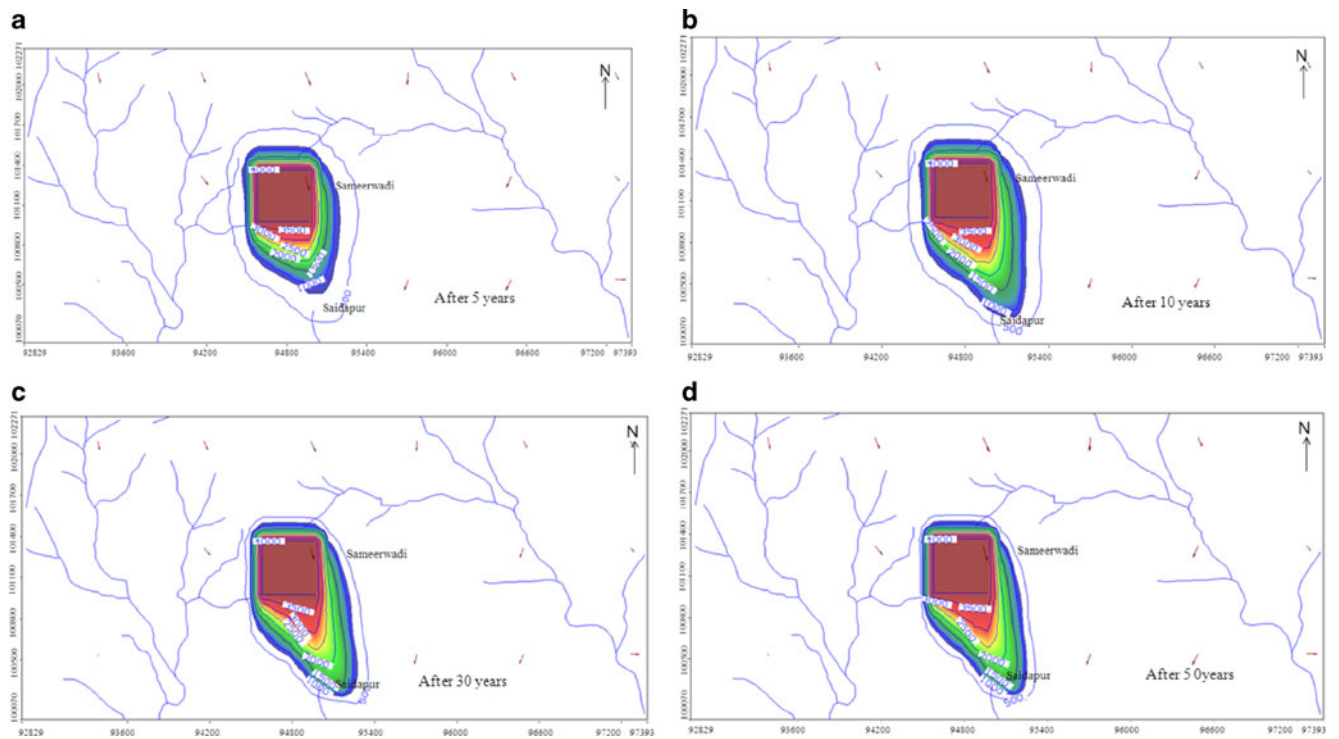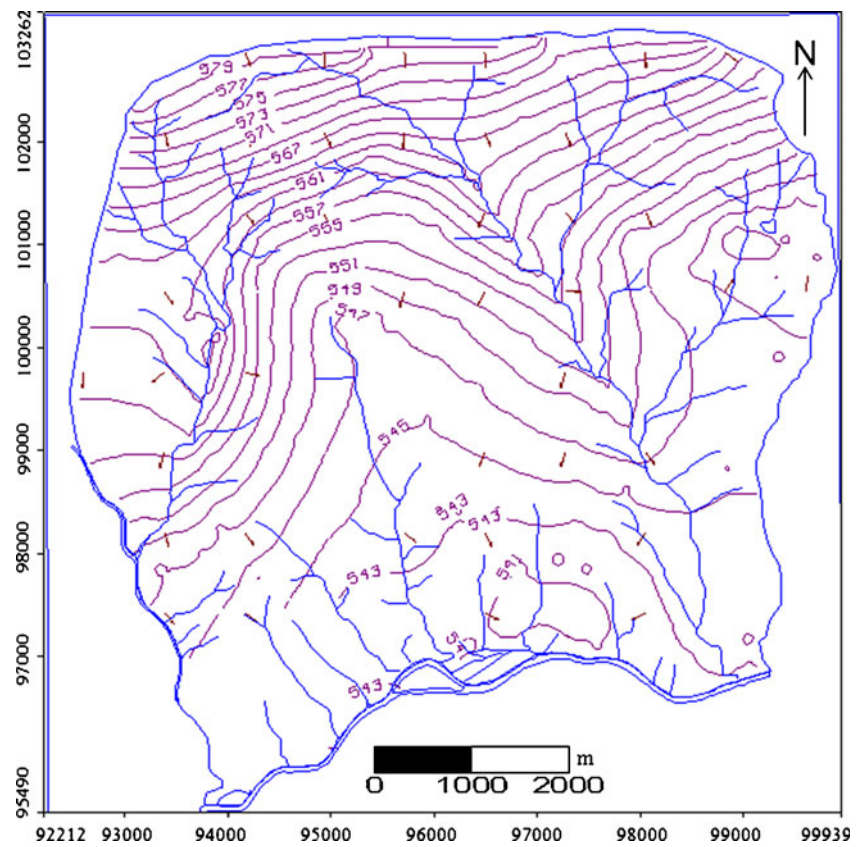
Fig. 11 Predicted contamination migration for different scenarios

Model results and discussions

The model estimated groundwater head distribution to reasonably agree with the regional groundwater contour map reconstructed from limited wellhead measurements. Unfortunately, piezometric data in the east, northeast, and west is scarce making comparison difficult in these areas. The computed groundwater level contours are showing the trend of observed water levels during July 2007(Fig. 10). It shows that water level contour is the subdued replica of the topographic surface.

The contaminant migration will be spreading in the downstream side up to a distance of about 125 m during next 5-year period in the unconfined first layer (Fig. 11a). The second layer, which mainly contains the vesicular zone, may attain a TDS concentration of 1,500 mg/L. The rapid downgradient movement of pollution coming from the peri-urban area of interest can be observed, thus seepage from the composting area shall be moving slowly through the top layer and once it reaches the second layer, it could move faster due to higher permeability of the formations. The predicted TDS plume could be migrated towards the downstream area with a distance of 250 m within the span of 10 years (Fig. 11b). The migration of TDS plume monitored in the present study if not intercepted at the initial stages is likely to magnify and further contaminate the groundwater reservoirs posing a major threat to the entire living community of the area. The predicted TDS plume would be migrated towards near Madbhavi village within 30 years (Fig. 11c). The contaminant plume coming from the study area spreads to the southern part. Factors like intercalation of basalt flows separated by baked soils, which form weak zones at the contact; the columnar joints of the basalt; the inclined bedding of most scoriaceous basalts; and fractures zones and their close spacing allow easy groundwater circulation and contaminant migration in the area. In addition, the characteristics of soil influences the amount of recharge infiltrating into the ground, the amount of potential dispersion, and the purifying process of contaminants to move vertically into the deeper zone. Therefore, even the black cotton soils which appear to be impermeable to infiltrations have of course relatively low permeability in the region but they are permeable to fluids. In addition, due to intensive erosional activities, there is poor soil development on most parts of the slope which proves the lack of defense line to hydrogeological system. Therefore, the danger zones are areas of rock exposures with no soil coverage and faulted zones. Thus, it is important to consider hydraulic conductivity of the scoriaceous basalt, which on average is 4 m/day. In that case, there is a possibility of arrival of pollutant to the well field. The results demonstrate how an early warning system could be established using the results of the groundwater modeling exercise; for instance, the effects of dumping of hazardous material of industrial locations could easily be tracked, allowing first arrival and peak concentration times to be predicted. Visualization of TDS migration in groundwater for 50 years has been presented (Fig. 11d). Even with the efforts made by Organo Chemicals Unit during the last few years by closing the existing lagoons and modernizing the compost area with thick clay layer, the contamination already reached up to nearby wells fields. This hypothesis was supported by investigations in the present, focused mainly in agricultural and industrial pollution, while the influence of the city itself was neglected. It was not entirely clear whether the exposed pollution originated from the agriculture and industry, or it is the result of growing urbanization.

Conclusion

This paper provides an improved understanding of the contaminate migration and the factors governing groundwater quality in a regional aquifer system. Groundwater chemistry is mainly controlled by silicate weathering in the study area. Higher concentration of TDS and NO_3-N are observed in the study area; due to domestic effluents, agriculture and local anthropogenic activities are directed into the groundwater, which would have increased the concentration of the ions in the water. Geophysical investigations have indicated that the composting area was located on high resistivity formation underlain by a low-resistivity formation. Though the effect of contaminant migration is currently minimal, the model developed in this study clearly shows that contamination of the well field is forthcoming, unless strong environmental protection policy as well as aquifer management strategy is implemented. Currently, the degree of contamination of the groundwater is negligible giving certain time to avert the problem. However, the model indicates that the migration of contamination would be reached in the nearby well field in less than 10 years. Flow is not linear throughout the system; rather, it is more rapid where porosity and transmissivity are high depending on the orientation of tectonic fractures.

References

Acworth RI (2001) The electrical image method compared with resistivity sounding and electromagnetic profiling for investigation in areas of complex geology—a case study from groundwater investigation in a weathered crystalline rock environment. Explor Geophys 32:119–128

Anderson MP, Woessner WW (1992) Applied groundwater modeling—simulation of flow and advective transport. Academic press, San Diego, CA, USA

APHA (1995) Standard methods for the examination of water and waste water (19th ed.). Washington D.C., American Public Health Association

Bakri S, Rahman L, Bowling L (2008) Sources and management of urban stormwater pollution in rural catchments, Australia. J Hydrol 356:299–311

Brown E, Skougstand MW, Fishman MJ (1970) Methods for collection and analyses of water samples for dissolved minerals and gases. Techniques of Water Resources Investigation of the US Geological Survey 5

Domenico PA, Schwartz FW (1990) Physical and chemical hydrology. Wiley, New York

Elango L, Kannan R (2007) Rock–water interaction and its control on chemical composition of groundwater. Chap. 11. Dev in Env Sci 5:229–243

Fogg GE, Noyes CD, Carle SF (1998) Geologically based model of heterogeneous hydraulic conductivity in an alluvial setting. Hydrogeol J 6:131–143

Foppen JWA (2002) Impact of high-strength wastewater infiltration on groundwater quality and drinking water supply: the case of Sana'a, Yemen. J Hydrol 263:198–216

Freeze RA, Cherry JA (1979) Groundwater. Prentice-Hall, Englewood Cliffs, NJ, USA, p 604

Gibbs R J (1970) Mechanisms controlling World's water chemistry. Science 170:1088–1090

Gobel P, Stubbe H, Weinert M, Zimmermann J, Fach S, Dierkes C, Kories H, Messer J, Mertsch V, Geiger WF, Coldewey WG (2004) Near-natural storm water management and its effects on the water budget and groundwater surface in urban areas taking account of the hydrogeological conditions. J Hydrol 299:267–283

GSI (1991) Geology and minerals resource map. Bagalkot District, Karnataka

Harbaugh AW, Banta ER, Hill MC, McDonald MG (2000) The US geological survey's modular ground water flow model e user guide to modularization concepts and the ground water flow process. US Geological Survey. Open-File Report 00e92

Janardhan Raju N (2007) Hydrogeochemical parameters for assessment of groundwater quality in the upper Gunjanaeru River basin, Cuddapah District, Andhra Pradesh, South India. Environ Geol 52:1067–1074. doi:10.1007/s00254-006-0546-0

Jat MK, Khare D, Garg PK (2009) Urbanization and its impact on groundwater: a remote sensing and GIS-based assessment approach. Environmentalist 29:17–32

Konikow LF, Bredehoeft JD (1978) Computer model of two-dimensional solute transport and dispersion in ground water, USGS, book 7, chapter C2, Washington, pp.90

Mahesha V, Prasannakumar D (1989) Groundwater resources of Hungund Taluk: a re-evaluation. Groundwater studies no. 234. Department of Mines and Geology, Bangalore, Karnataka

McDonald JM, Harbaugh AW (1988) A modular three-dimensional finite-difference groundwater flow model. Techniques of water resources investigations of the US Geological Survey Book.6, pp. 586

Mitchell VG, Duncan H, Inma, Rahilly M, Stewart J, Vieritz A, Holt P, Grant A, Fletcher TD, Coleman J, Maheepala S, Sharma A, Deletic A, Breen P (2007) State of the art review of integrated urban water models. In: Novatech Lyon, France, pp.1–8

Rao VVSG, Prakash B A, Ramesh M, Ramesh G, Tamma Rao G, Surinaidu, L, Mahesh J (2008) Assessment of groundwater conditions & contaminant migration in groundwater in the watersheds covering M/s. Somaiya Organo Chemicals, a Unit of Godavari Sugar Mills Limited, Sameerwadi, Bhagalkot district, Karnataka. No. NGRI-2008-Environ-638, p. 22

Shepherd KA, Ellis PA, Rivett MO (2006) Integrated understanding of urban land, groundwater, baseflow and surface-water quality—the city of Birmingham, UK. Sci Total Environ 360:180–195

Singh VK, Bikundia DS, Sarswat A, Mohan D (2011) Groundwater quality assessment in the village of Lutfullapur Nawada, Loni, District Ghaziabad, Uttar Pradesh, India. Environ Monit Assess. doi:10.1007/s10661-011-2279-0

Srinivasamoorthy K, Chidambaram S, Prasanna MV, Vasanthavihar M, John P, Anandhan P (2008) Identification of major sources controlling groundwater chemistry from a hard rock terrain—a case study from Mettur taluk, Salem district, Tamil Nadu, India. J Earth Syst Sci 117:49–58

Stallard R, Edmond JM (1983) Geochemistry of the Amazon. 2. The influence of geology and weathering environment on the dissolved load. J Geophys Res 88:9671–9688

Vidal M, Melgar J, Lopez A, Santoalla MC (2000) Spatial and temporal hydrochemical changes in groundwater under the contaminating effects of fertilizers and wastewater. J Environ Manag 60:215–225

Wolf L (2007) Managing urban groundwater as a resource—hidden problems and hidden opportunities. Water 21:21–25

Zheng C (1990) MT3D, a modular three-dimensional transport model for simulation of advection, dispersion and chemical reactions of contaminants in groundwater system prepared for the US Envi Prot Agency

Zheng C, Wang P (1999) MT3DMS: a modular three-dimensional multispecies transport model for simulation of advection, dispersion, and chemical reactions of contaminants in ground-water systems, documentation and user's guide. US Army Corps of Engineers, Washington, DC